

DFTT 04/05
 IFUP-TH 2005-04
 DIAS-STP-05-01

Comparing the Nambu–Goto string with LGT results

M. Caselle^a, M. Hasenbusch^b and M. Panero^c

^a *Dipartimento di Fisica Teorica dell’Università di Torino and I.N.F.N.,
 via P.Giuria 1, I-10125 Torino, Italy
 e-mail: caselle@to.infn.it*

^b *Dipartimento di Fisica dell’Università di Pisa and I.N.F.N.,
 Largo Bruno Pontecorvo 3, I-56127 Pisa, Italy
 e-mail: Martin.Hasenbusch@df.unipi.it*

^c *School of Theoretical Physics, Dublin Institute for Advanced Studies,
 10 Burlington Road, Dublin 4, Ireland
 e-mail: panero@stp.dias.ie*

Abstract

We discuss a way to evaluate the full prediction for the interquark potential which is expected from the effective Nambu–Goto string model. We check the correctness of the prescription reproducing the results obtained with the zeta function regularization for the first two perturbative orders. We compare the predictions with existing Monte Carlo data for the (2+1) dimensional \mathbb{Z}_2 , $SU(2)$ and $SU(3)$ gauge theories: in the low temperature regime, we find good agreement for large enough interquark distances, but an increasing mismatch between theoretical predictions and numerical results is observed as shorter and shorter distances are investigated. On the contrary, at high temperatures (approaching the deconfinement transition from below) a remarkable agreement between Monte Carlo data and the expectations from the Nambu–Goto effective string is observed for a wide range of interquark distances.

1 Introduction

Working out an effective string description for the infrared behaviour of the interquark potential is one of the major challenges of modern lattice gauge theory [1–3]. In these last years, much effort has been devoted in trying to identify the nature of an effective string model that reproduces the results of high precision numerical studies of the confining potential in pure gauge models [4]–[23]. Despite these efforts, a clear answer has not been obtained yet. The simplest, and most natural, candidate for an effective string picture is the Nambu–Goto model [25–27]: numerical tests of the predictions of this model at the first leading orders, however, did not lead to conclusive results. As a matter of fact, the data obtained for different lattice gauge theories at short interquark distances R disagree with the Nambu–Goto predictions [11–14], whereas at large distances the agreement is remarkably good [10–12].

In the setting where one considers a confined, static, quark-antiquark ($Q\bar{Q}$) pair at a finite temperature T , a possible way to derive effective predictions from the Nambu–Goto model consists in working out a perturbative expansion in powers of $(\sigma RL)^{-1}$, a dimensionless quantity which depends on the interquark distance R , on the system size in the compactified direction L (which is inversely proportional to the temperature) and on the string tension σ . As it is expected, the leading, non-trivial (LO) contribution emerging in this expansion describes the asymptotic free string picture, whose degrees of freedom are independent, massless bosons associated with string vibrations along the transverse directions, whose partition function can be easily evaluated by means of standard conformal field theory techniques. The contribution at the next-to-leading order (NLO) can also be evaluated analytically [3], but treating further terms in such a perturbative expansion would be much more difficult. On the other hand, comparison of numerical results with the next-to-leading-order predictions can be tricky, as it is difficult to judge if the mismatch observed, for instance, at short distances and low temperatures could be interpreted as an effect due to the NLO truncation, or if — *vice versa* — the agreement which is found at high temperatures could be spoiled by higher orders (see discussion in section 5 of [10]).

Here we address this problem by estimating the full partition function of the Nambu–Goto effective string model, relying on the fact that formal quantization of this model is possible, and the spectrum can be obtained analytically [24]. This procedure allows for a comparison with the existing Monte Carlo data of the interquark potential that is not biased by the truncation effects discussed above.

The results of this comparison can be summarized as follows:

- The mismatch between numerical data and NLO predictions which is observed at short distances is confirmed (and even enhanced) if one considers the full string prediction.
- On the contrary, at higher temperatures, approaching the deconfinement transition from below, a remarkable agreement (which is particularly striking for the case of

$SU(2)$ gauge group) between Monte Carlo data and full Nambu–Goto expectations is found.

These observations suggest that the Nambu–Goto action does not provide a correct description of the interquark potential at short distances, where an alternative effective model is probably needed. At the same time, however, they also suggest that this effective string action can be considered as a reliable (and better than the pure “free string picture”) description of the interquark potential at large distances. As the finite-temperature deconfinement transition is approached we observe a crossover between this “universal” Nambu–Goto behaviour and a new behaviour which is different in the \mathbb{Z}_2 and $SU(2)$ cases and keeps into account the fact the Nambu–Goto action would lead to the wrong critical indices at the deconfinement point.

This paper is organized as follows. In section 2, after recalling the basics about the Nambu–Goto model, we work out the predictions of interest for the effective string scenario, using the perturbative approach and evaluating the full partition function in terms of the string spectrum. We also comment about the convergence bounds that naturally arise in the latter approach. In section 3, the predictions of the full string partition function are compared with existing Monte Carlo data for \mathbb{Z}_2 , $SU(2)$ and $SU(3)$ LGT in $(2+1)$ dimensions. Finally, in section 4 we summarize the results and provide our conclusions. Calculations displaying the matching between the full partition function and the known perturbative results at leading and next-to-leading order are reported in the Appendix.

2 The Nambu–Goto string

In this section, we report some results concerning the Nambu–Goto string model [25–27] which will be useful to our analysis. We refer the reader to [10] for a more detailed derivation. The action of this model is proportional to the area of the string world-sheet:

$$S = \sigma \int_0^L d\tau \int_0^R d\varsigma \sqrt{g} \ , \quad (1)$$

where g is the determinant of the two-dimensional metric induced on the world-sheet by the embedding in R^d and σ is the string tension, which appears as a parameter of the effective model.

Eq. (1) is invariant with respect to reparametrization and Weyl transformations, and a possible choice for quantization of the effective model is the “physical gauge” (see [2] for more details) in which g becomes a function of the transverse displacements of the string world-sheet only. The latter (which can be denoted as $X^i(\tau, \varsigma)$) are required to satisfy the boundary conditions relevant to the problem — in the present case, the effective string world-sheet associated with a two-point Polyakov loop correlation function obeys periodic b.c. in the compactified direction and Dirichlet b.c. along the interquark axis direction:

$$X^i(\tau + L, \varsigma) = X^i(\tau, \varsigma); \quad X^i(\tau, 0) = X^i(\tau, R) = 0 \ . \quad (2)$$

This gauge fixing implicitly assumes that the world-sheet surface is a single-valued function of (τ, ς) , i.e. overhangs, cuts, or disconnected parts are excluded. It is well known that rotational symmetry of this model is broken at a quantum level because of the Weyl anomaly, unless the model is defined in the critical dimension $d = 26$. However, this anomaly is known to be vanishing at large distances [30], and this suggests to use the “physical gauge” for an IR, effective string description also for $d \neq 26$.

Here and in the following, we restrict our attention to the $d = 2 + 1$ case, which is particularly simple, as there is only one transverse degree of freedom (X). In the physical gauge, eq. (1) takes the form:

$$S[X] = \sigma \int_0^L d\tau \int_0^R d\varsigma \sqrt{1 + (\partial_\tau X)^2 + (\partial_\varsigma X)^2} . \quad (3)$$

This action describes a non-renormalizable, interacting QFT in two dimensions; the associated partition function is expected to encode an effective description for this sector of the gauge theory, providing a prediction for the VEV of the two-point Polyakov loop correlation function:

$$\langle P^\dagger(R)P(0) \rangle = Z = \int \mathcal{D}X e^{-S[X]} . \quad (4)$$

Quantum corrections beyond the classical solution (which corresponds to a flat string world-sheet surface) can be studied in two different ways.

2.1 Perturbative expansion of the partition function

Despite the fact that the Nambu–Goto string theory is non-renormalizable, one can address the study of the effective model in a perturbative way, expanding the square root appearing in eq. (3) in powers of the dimensionless quantity $(\sigma RL)^{-1}$: this approach is expected to be consistent with the fact that the effective theory holds in the IR regime of the confined phase.

Going to dimensionless world-sheet coordinates: $\xi_1 = \tau/L$, $\xi_2 = \varsigma/R$ and with a global rescaling for the X field: $\phi = \sqrt{\sigma}X$, eq. (3) can then be expanded in a natural way in a series of terms associated with different powers of $(\sigma RL)^{-1}$; in particular, the first few terms read:

$$S = \sigma LR + \frac{1}{2} \int_0^1 d\xi_1 \int_0^1 d\xi_2 (\nabla\phi)^2 - \frac{1}{8\sigma LR} \int_0^1 d\xi_1 \int_0^1 d\xi_2 [(\nabla\phi)^2]^2 + O((\sigma RL)^{-2}) , \quad (5)$$

where:

$$(\nabla\phi)^2 = \frac{1}{2u} \left(\frac{\partial\phi}{\partial\xi_1} \right)^2 + 2u \left(\frac{\partial\phi}{\partial\xi_2} \right)^2 \quad (6)$$

and:

$$u = \frac{L}{2R} . \quad (7)$$

Apart from the trivial, classical contribution given by the first term appearing on the r.h.s. of eq. (5) — the second term of the expansion shows that the leading order quantum correction is nothing but the CFT of a free, massless bosonic field, while the subsequent $O((\sigma RL)^{-1})$ contribution (which is quartic in ϕ) encodes string self-interaction.

Discarding the string self-interaction term, the LO approximation of the partition function can be evaluated analytically:

$$Z^{LO}(L, R) = e^{-\sigma RL} \cdot Z_1 \quad , \quad (8)$$

where Z_1 encodes the (regularized) contribution of the Gaussian fluctuations:

$$Z_1 = \frac{1}{\eta(iu)} \quad (9)$$

and it is expressed in terms of Dedekind's η function:

$$\eta(\tau) = q^{\frac{1}{24}} \prod_{n=1}^{\infty} (1 - q^n) \quad ; \quad q = e^{2\pi i \tau} \quad , \quad (10)$$

On the other hand, keeping into account the string self-interaction term, the resulting approximation for Z at the next-to-leading order reads [3]:

$$Z^{NLO}(L, R) = e^{-\sigma RL} \cdot Z_1 \cdot \left\{ 1 + \frac{\pi^2 L}{1152\sigma R^3} [2E_4(iu) - E_2^2(iu)] \right\} \quad , \quad (11)$$

where E_2 and E_4 are the Eisenstein functions:

$$E_2(\tau) = 1 - 24 \sum_{n=1}^{\infty} \sigma_1(n) q^n \quad (12)$$

$$E_4(\tau) = 1 + 240 \sum_{n=1}^{\infty} \sigma_3(n) q^n \quad (13)$$

$$q = e^{2\pi i \tau} \quad , \quad (14)$$

where $\sigma_1(n)$ and $\sigma_3(n)$ are, respectively, the sum of all divisors of n (including 1 and n), and the sum of their cubes.

2.2 The string spectrum

The spectrum of the Nambu–Goto string with length R and fixed ends can be obtained through formal canonical quantization [24], and in $d = 2 + 1$ dimensions it reads:

$$E_n(R) = \sigma R \sqrt{1 + \frac{2\pi}{\sigma R^2} \left(n - \frac{1}{24} \right)} \quad , \quad n \in \mathbb{N} \quad . \quad (15)$$

The full partition function of the Nambu–Goto string can thus be written as — see also [6]:

$$Z = \sum_{n=0}^{\infty} w_n e^{-E_n L} \quad (16)$$

with integer weights w_n accounting for level multiplicities. In particular, in $d = 2 + 1$ the latter are nothing but $P(n)$: the number of partitions of n . In fact, since the w_n coefficients do not depend on R , they can be evaluated in the large R limit, where the theory eventually reduces to a $c = 1$ CFT in two dimensions. The Hilbert space of such a theory is well known and the multiplicity of states with energy E_n is given by the number of ways one can combine the Virasoro generators of the 2d conformal algebra to obtain a field of conformal weight n — which is precisely $P(n)$.

In principle, eq. (16) can provide a tool to test the validity range of the effective Nambu–Goto string picture, disentangling truncation errors which affect the perturbative expansion of Z , from physical effects related to the eventual breakdown of this effective string description at some scale.

In turn, it can be shown that the energy levels appearing in eq. (16) can be treated in a perturbative expansion in powers of $(\sigma R^2)^{-1}$, and the corresponding truncated approximations for $Z(R, L)$ correctly reproduce eq. (8) at LO (see also [6]) and eq. (11) at NLO (calculations are reported in the Appendix).

It is particularly interesting to study the domain of convergence of the series in (16).

For large n , the asymptotic behaviour of $P(n)$ is [28]:

$$P(n) \sim \frac{1}{4n\sqrt{3}} e^{\pi\sqrt{\frac{2n}{3}}} . \quad (17)$$

Thus, the series on the r.h.s. of eq. (16) turns out to be convergent for:

$$\frac{1}{\sigma L^2} < \frac{3}{\pi} . \quad (18)$$

On the other hand, a convergence constraint over R can be worked out exploiting the open-closed string duality to rewrite $Z(R, L)$ as a series of Bessel functions [6]:

$$\sum_{n=0}^{\infty} P(n) e^{-E_n(R)L} = \sqrt{\frac{\sigma L^2}{\pi}} \sum_{n=0}^{\infty} P(n) K_0(\tilde{E}_n R) \quad (19)$$

involving $\tilde{E}_n = \tilde{E}_n(L)$, the closed string energies:

$$\tilde{E}_n(L) = \sigma L \sqrt{1 + \frac{8\pi}{\sigma L^2} \left(n - \frac{1}{24} \right)} . \quad (20)$$

Since the asymptotic behaviour of $K_0(x)$ for large values of x is:

$$K_0(x) \sim \sqrt{\frac{\pi}{2x}} e^{-x} \left[1 + O\left(\frac{1}{x}\right) \right] \quad (21)$$

the series on the r.h.s. of (19) converges for:

$$\frac{1}{\sigma R^2} < \frac{12}{\pi} . \quad (22)$$

Let us comment on the constraints (18) and (22):

- They can be obtained from each other via interchanging $2R$ and L : this “symmetry” is related to the open-closed string duality.
- They can also be derived by requiring that the ground state energies for the open and closed string energies are real; in particular, inequality (18) — which was derived requiring convergence for the series involving *open* string states — can be obtained imposing that the *closed* string ground state energy is real, while inequality (22) — which, *vice versa*, was obtained requiring convergence of the series involving the *closed* string spectrum — can be obtained imposing that the *open* string ground state is real.
- These bounds are the analogue of the Hagedorn temperature in string thermodynamics.
- The bound of eq.(18) can be interpreted as a prediction for the deconfinement temperature [31,32] leading to the estimate $T_c = \sqrt{\frac{3\sigma}{\pi}}$, which is in rather good agreement with the results of numerical simulations for various lattice gauge theories in $d = 2+1$.
- The inequality (22) implies a lower bound for the interquark distance at which the Nambu-Goto string could be observed: $\sigma R_c^2 > \frac{\pi}{12} \sim 0.262\dots$. In physical units¹ R_c is slightly below 0.1 fm (as it can be easily seen comparing it with the so called “Sommer scale” R_s defined by the relation $F(R_s)R_s^2 = 1.65$ [15] which corresponds to a physical length $R_c \simeq 0.5$ fm). However this bound is less relevant from a physical point of view than the previous one since, as we shall see below, the MC results for the interquark potential start to diverge from the predictions of the Nambu-Goto action at distances much larger than R_c .

3 Comparison with Monte Carlo simulations

Before presenting the comparison of theoretical predictions with the numerical results for various gauge models, let us discuss a few aspects about the evaluation of the partition function appearing in eq. (4) by means of eq. (16).

The sum of the series in eq. (16) cannot be evaluated in closed form and its numerical estimate is not completely trivial, since both rounding and truncation effects must be kept under control.

¹Note that the length scale refers to QCD in 3+1 dimensions.

Calculating the partitions of the integers $P(n)$ appearing as coefficients in eq. (16) is a task that can be addressed in an efficient way without resorting to any commercial program by means of the following identity:

$$P(n) = \sum_{k=1}^n P_k(n) \quad (23)$$

where $P_k(n)$ denotes the number of partitions of n made exactly of k parts, which enjoys the recursive relation [29]:

$$P_k(n) = P_{k-1}(n-1) + P_k(n-k) . \quad (24)$$

To avoid truncation errors one can use from a given threshold n_{max} the approximation of eq.(17) for the weights $P(n)$ and then approximate the sum for $n > n_{max}$ in the partition function with an integral. We checked that for all the choices of σ , R and L that we studied $n_{max} = 10000$ was enough to keep the systematic errors of our estimates several orders of magnitude smaller than the statistical uncertainties of the MC estimates of the same quantities.

3.1 \mathbb{Z}_2 gauge model

As a first test, we considered the results for \mathbb{Z}_2 gauge model in $d = 2 + 1$ taken from [10] and [11] — to which we refer the reader for notations and general properties of this lattice gauge theory. In addition to these data we also performed some new simulations whose results are collected in tab. 5. In the present analysis, we focus the attention onto the data samples corresponding to the coupling parameter $\beta = 0.75180$ (which is the nearest to the critical point, among the values studied in the mentioned papers), for which the finite temperature deconfinement transition occurs at $L_c = 8$ [33]. For the samples that we considered here, the temperatures range from $T = \frac{T_c}{10}$ to $T = \frac{2}{3}T_c$. For the zero temperature string tension at this value of β , we used the estimate given in [11]: $\sigma = 0.0105241(15)$ which was obtained from our data sample at $T = \frac{T_c}{10}$, i.e. $L = 80$ and $R \geq 22$, taking into account LO order corrections only. The numbers given in table 1 show that subleading corrections are of a similar size as the statistical errors of our Monte Carlo data for these large values of L and R .

In our analysis, we did not consider effects induced by a possible “boundary term” that could be included in the effective string action [5], since numerical results in [11] and [12] already showed that the coefficient of such a term is vanishing for this model, and, from the theoretical point of view, the presence of a boundary term in the string action is ruled out, if open-closed string duality holds [6].

For this value of β we expect very small scaling corrections to our data. In [11] we directly verified this by comparing our results for $\beta = 0.75180$ with those taken at $\beta = 0.73107$ (corresponding to a string tension which is roughly four times larger than here). An independent check is given by the product σL_c^2 . For the value of β we study here, one

finds $\sigma L_c^2 = 0.6740(10)$, which deviates from the asymptotic estimate $\sigma L_c^2 = 0.654(3)$ less than 3% [34].

The results of our analysis are shown in tables 1–5, where Monte Carlo results for the ratio $\Gamma(R) = \frac{G(R+1)}{G(R)}$ (rightmost column) are compared with the corresponding predictions from the LO-truncated, NLO-truncated, or full effective Nambu–Goto string, obtained from eq. (8), from eq. (11), and from eq. (16), respectively.

All these theoretical estimates are affected by an uncertainty (due to the statistical error in σ , and proportional to σL^2) whose relative amount is of order 10^{-5} (for $L = 12$) or 10^{-4} (for $L = 80$), and it is never larger than the statistical errors of the Monte Carlo data. For this reason, we chose not to report this overall uncertainty in the tables, in order to avoid confusion.

We remark the fact that the comparison is “absolute”, in the sense that there is no free parameter.

The results can be summarized as follows.

- For the two samples at the lowest temperatures ($T = \frac{T_c}{10}$ and $T = \frac{T_c}{3}$), Monte Carlo data and theoretical estimates obtained from the full partition function are in good agreement for $R \geq 30$ and $R \geq 24$, respectively. However, it is also important to notice that in this range the NLO-truncated predictions show no substantial difference with respect to the estimates from the complete action. Conversely, for lower values of R , the numerical data are not compatible with predictions from either eq. (8), eq. (11), or from eq. (16): in that regime, the Monte Carlo results for $\Gamma(R)$ appear to be systematically larger than the values predicted by the effective string picture, and, in particular, the discrepancy gets even larger when R decreases. This mismatch had already been observed in [11], using the NLO-truncation. Here, we find that keeping into account the subleading corrections from the whole Nambu–Goto action does not remove the disagreement².
- For the two samples at higher temperatures ($T = \frac{T_c}{2}$ and $T = \frac{2}{3}T_c$), the contribution by subleading terms beyond the NLO becomes quantitatively more relevant and the precision of the numerical data allows to appreciate the difference between the predictions of eq. (11) and eq. (16) for all values of R that are considered.

For $T = \frac{T_c}{2}$ and $R \geq 16$, the Monte Carlo data lie in between the full Nambu–Goto expectation and the NLO truncation. For $T = \frac{T_c}{2}$ and $R \geq 16$, the Monte Carlo data fall (incidentally), within about two standard deviations, on top of the NLO truncation. The numerical matching with the full Nambu–Goto is clearly worse.

- It is very interesting to look at the data at fixed $R = 32$ collected in tab. 5. We see that for all values of $L > 16$ the data agree with the Nambu–Goto predictions almost within one standard deviation. Fortunately in this region the precision is high enough to distinguish between LO, NLO and full Nambu–Goto. The picture which

²Quantitatively, the subleading corrections induce an even larger mismatch.

emerges, in agreement with the above observation is that the Nambu–Goto string is the correct description for low enough temperatures and that around $T = T_c/2$ there is a smooth crossover towards a behaviour which is instead very near to the NLO result. We shall discuss in more detail this point in the last section.

R	LO	NLO	full NG	MC data
8	0.372554	0.358712	0.353033	0.382613(58)
10	0.391751	0.385458	0.383979	0.396313(61)
12	0.402904	0.399676	0.399177	0.405088(65)
14	0.409919	0.408105	0.407905	0.411017(69)
16	0.414606	0.413511	0.413422	0.415268(71)
18	0.417886	0.417189	0.417146	0.418048(74)
20	0.420270	0.419808	0.419786	0.420344(74)
22	0.422056	0.421741	0.421730	0.422062(78)
24	0.423430	0.423211	0.423205	0.423323(78)
26	0.424511	0.424357	0.424354	0.424486(78)
28	0.425377	0.425270	0.425269	0.425496(81)
30	0.426085	0.426012	0.426011	0.425958(81)
32	0.426672	0.426624	0.426624	0.426747(82)
36	0.427588	0.427574	0.427573	0.427513(83)
40	0.428270	0.428276	0.428274	0.428255(84)
60	0.430134	0.430159	0.430158	0.430097(87)
80	0.431023	0.431043	0.431043	0.431068(88)

Table 1: Comparison of Monte Carlo results (last column) for correlator ratios $\Gamma(R) = \frac{G(R+1)}{G(R)}$ in the \mathbb{Z}_2 gauge model at $\beta = 0.75180$ and $T = \frac{T_c}{10}$ (corresponding to $L = 80$) with the LO-truncated, NLO-truncated, and full predictions from the Nambu–Goto effective string action (respectively: second, third, and fourth column), as a function of the interquark distance in lattice units R (first column). Note that the data for $R \geq 22$ were used in ref. [11] to determine the value of σ which is used here; assuming LO corrections.

3.2 $SU(2)$ gauge model

For the $SU(2)$ model in $d = 2+1$ dimensions we considered data published in [12] (to which we refer the reader for details and notation), focusing onto the two samples corresponding to the largest ($L = 60$) and the smallest ($L = 8$) values the inverse temperature at $\beta = 9.0$ — the other samples reported in [12] show the same qualitative behaviour which is observed for the data set at $L = 60$, adding no further information to the present analysis.

For $\beta = 9.0$ the string tension of this model is known to a high degree of precision: $\sigma = 0.025900(12)$ [12]. The lower bound R_c is between 3 and 4 lattice spacings and the

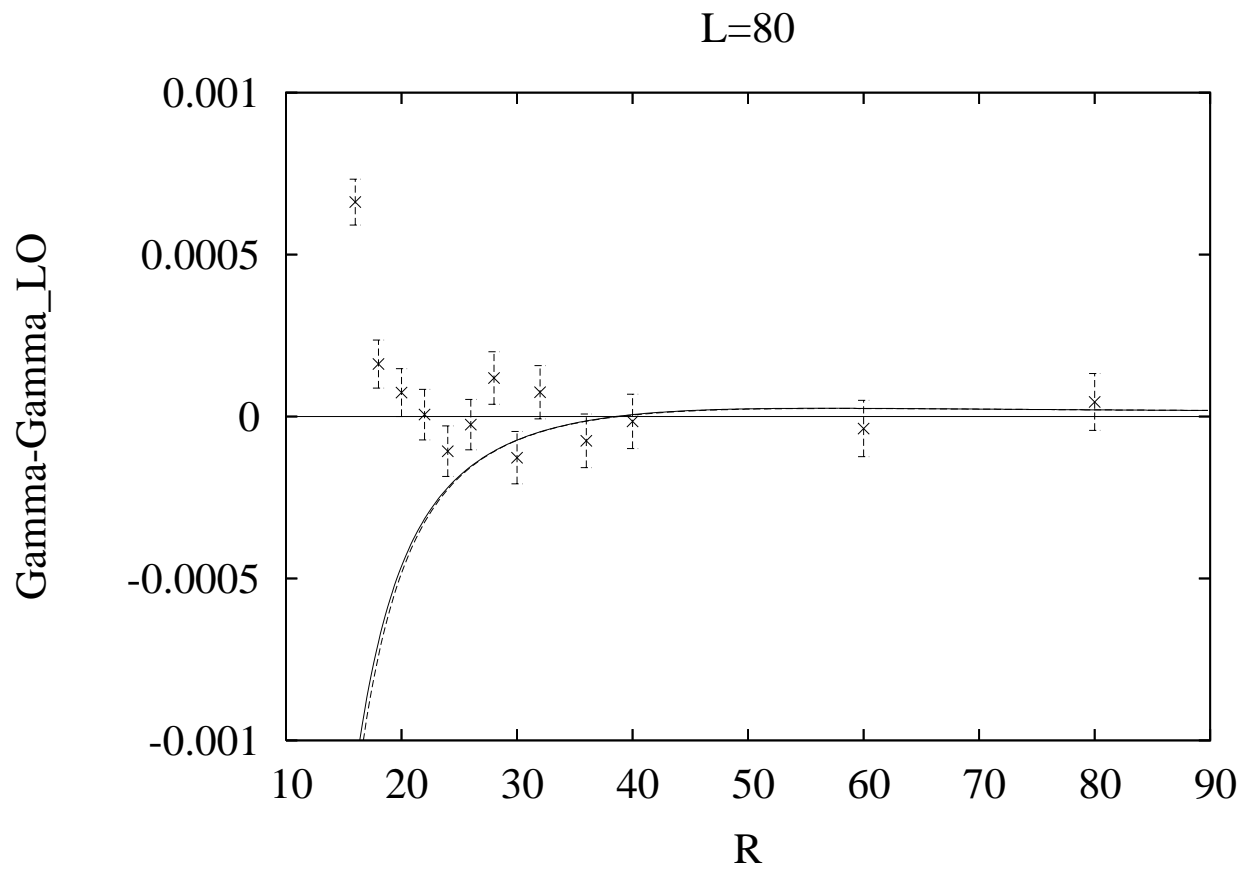


Figure 1: Differences between the values of $\Gamma(R)$ for the full Nambu–Goto action (dashed line), the NLO approximation (solid line) and the Monte Carlo results (crosses) with respect to the LO approximation for the sample at $\beta = 0.75180$, $L = 80$ in the Ising gauge model (data of tab. 1). Notice that for this value of L the NLO and full Nambu–Goto results almost coincide and cannot be separated in the figure.

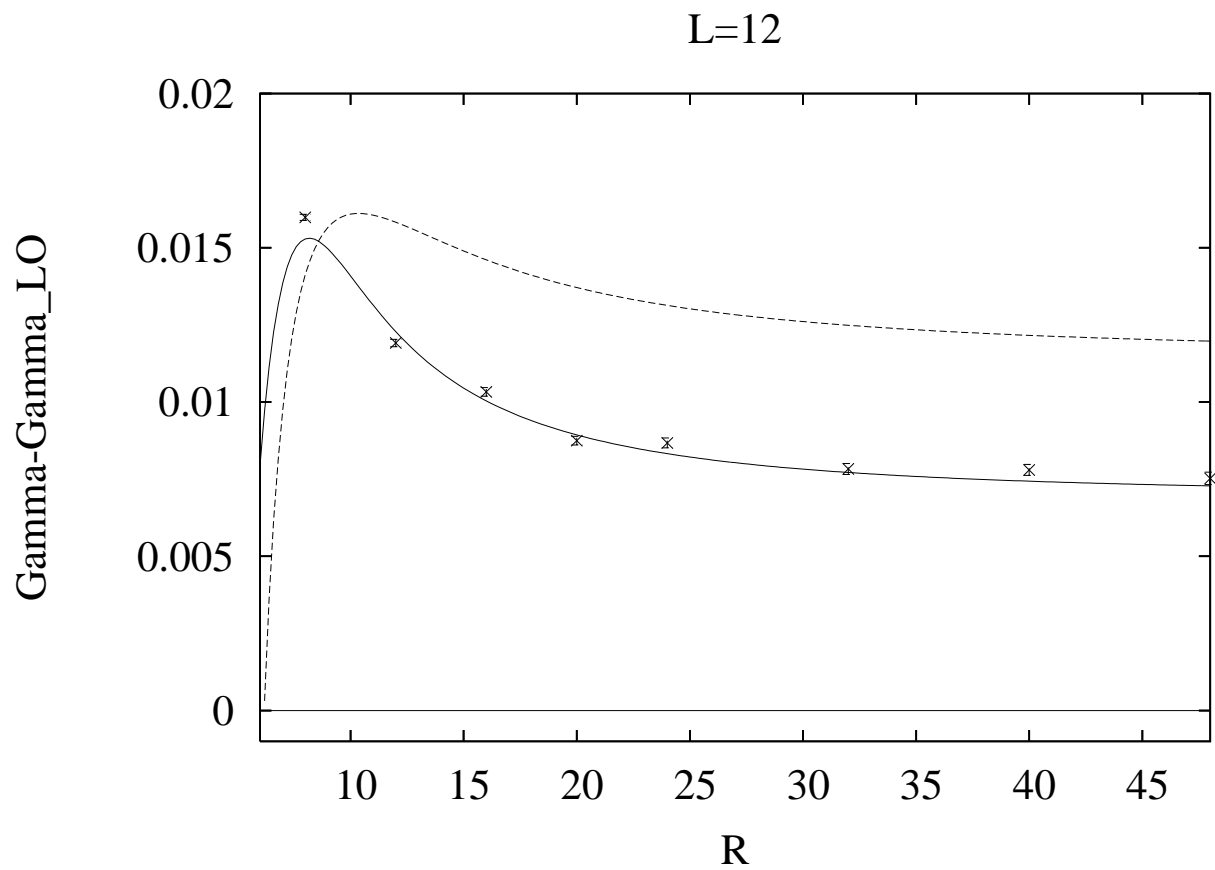


Figure 2: Same as fig. 1 but for the data at $L = 12$ (see tab. 4). In this case the difference between NLO and full Nambu–Goto predictions is perfectly detectable.

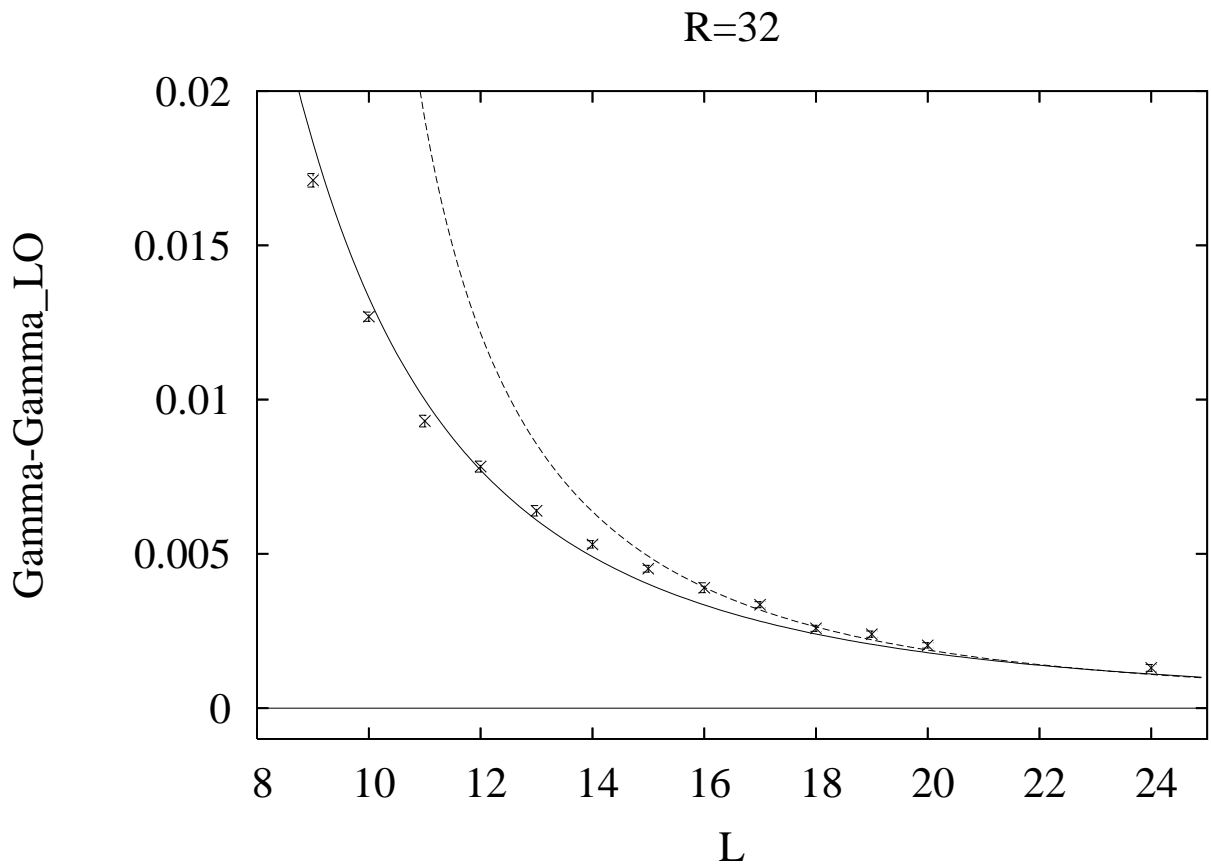


Figure 3: Same as fig. 1, but for the data at $R = 32$ (see tab. 5). As mentioned in the text, in this case the Monte Carlo results appear to interpolate between the full Nambu-Goto behaviour (dashed line) at low temperature and the NLO one (solid line) at high temperature.

R	LO	NLO	full NG	MC data
8	0.74374	0.73654	0.73364	0.75075(7)
12	0.76220	0.76282	0.76223	0.76492(8)
16	0.77015	0.77183	0.77150	0.77193(8)
20	0.77479	0.77636	0.77625	0.77661(9)
24	0.77789	0.77925	0.77925	0.77926(10)
32	0.78181	0.78291	0.78297	0.78311(11)
40	0.78419	0.78516	0.78523	0.78532(12)
48	0.78578	0.78669	0.78677	0.78677(13)

Table 2: *Same as in table 1, but for $T = \frac{T_c}{3}$ ($L = 24$).*

R	LO	NLO	full NG	MC data
8	0.82236	0.82516	0.82161	0.83207(8)
12	0.83885	0.84492	0.84415	0.84523(9)
16	0.84707	0.85205	0.85233	0.85220(10)
20	0.85210	0.85632	0.85693	0.85655(12)
24	0.85550	0.85928	0.85999	0.85937(13)
32	0.85981	0.86315	0.86390	0.86371(16)
40	0.86242	0.86556	0.86631	0.86624(15)
48	0.86418	0.86721	0.86796	0.86740(17)

Table 3: *Same as in table 1, but for $T = \frac{T_c}{2}$ ($L = 16$).*

deconfinement temperature in lattice units is approximately $T_c \simeq \frac{1}{6}$, thus the two samples that we are considering correspond to $T = \frac{T_c}{10}$ and $T = \frac{3}{4}T_c$ respectively. In agreement with notations in [12], we define the following quantity:

$$Q(R) = -\frac{1}{L} \log \left(\frac{G(R+1)}{G(R)} \right) \quad (25)$$

whose dominant contribution is the string tension; the relative error induced by the uncertainty in σ is approximately of order 10^{-4} , which turns out to be negligible or comparable with respect to the Monte Carlo result precision for both samples.

Comparison between numerical data and theoretical expectations is reported in tables 6, 7, with the same format used for previous tables.

The results for this model show that:

- At low temperatures, the behaviour of Monte Carlo data for $SU(2)$ is very similar to the \mathbb{Z}_2 gauge model; in particular, the lattice simulation results disagree with respect to the predictions from the full Nambu–Goto partition function, whose subleading

R	LO	NLO	full NG	MC data
8	0.86788	0.88317	0.88202	0.88387(10)
12	0.88455	0.89683	0.90037	0.89646(12)
16	0.89318	0.90322	0.90779	0.90351(14)
20	0.89848	0.90741	0.91219	0.90723(14)
24	0.90207	0.91039	0.91520	0.91074(16)
32	0.90661	0.91433	0.91910	0.91444(18)
40	0.90937	0.91680	0.92153	0.91717(18)
48	0.91122	0.91851	0.92320	0.91875(20)

Table 4: *Same as table 1, but for $T = \frac{2}{3}T_c$ (corresponding to $L = 12$).*

terms with respect to the NLO-truncated approximation induce an increasing gap between numerical data and theoretical expectations as shorter and shorter interquark distances are investigated.

- On the contrary, for the high temperature ($T = \frac{3}{4}T_c$) sample, $SU(2)$ results are in remarkable agreement with the predictions of the full Nambu–Goto partition function: agreement within statistical errors is observed for all interquark distances $R > 6$. Notice that in this temperature regime the subleading string effects play a relevant role, and the LO, NLO and full Nambu–Goto predictions can be clearly distinguished within the precision of numerical data: in particular, the difference between the full-order prediction and the NLO approximation is larger than five times the uncertainty of Monte Carlo data, for all values of R .

3.3 $SU(3)$ gauge model

For the $SU(3)$ model in $d = 2+1$ dimensions, we compare the theoretical expectations with the data published in [5]. We focused onto the sample at $\beta = 20$, using the data reported in tab. 3 of [5] to build the $Q(R)$ observable discussed above³. In this case we have $L = 60$, corresponding to a temperature $T \simeq \frac{T_c}{10}$, while we have no data for the high T regime. An estimate for the string tension σ can be obtained from the data themselves, following a procedure similar to the one used in [12] for the $SU(2)$ model; we found $\sigma = 0.033754(3)$, corresponding to a lower bound R_c between 2 and 3 lattice spacings.

Comparison of theoretical predictions and numerical data is reported in table 8, in the same format used for the previous cases. The pattern which emerges is the same that is observed for $SU(2)$ at low temperatures, the only difference being that the mismatch between the full Nambu–Goto string prediction and Monte Carlo results appears to be slightly smaller than in the $SU(2)$ case.

³Notice the shift in R between our $Q(R)$ and the quantity $F(R)$ in [5].

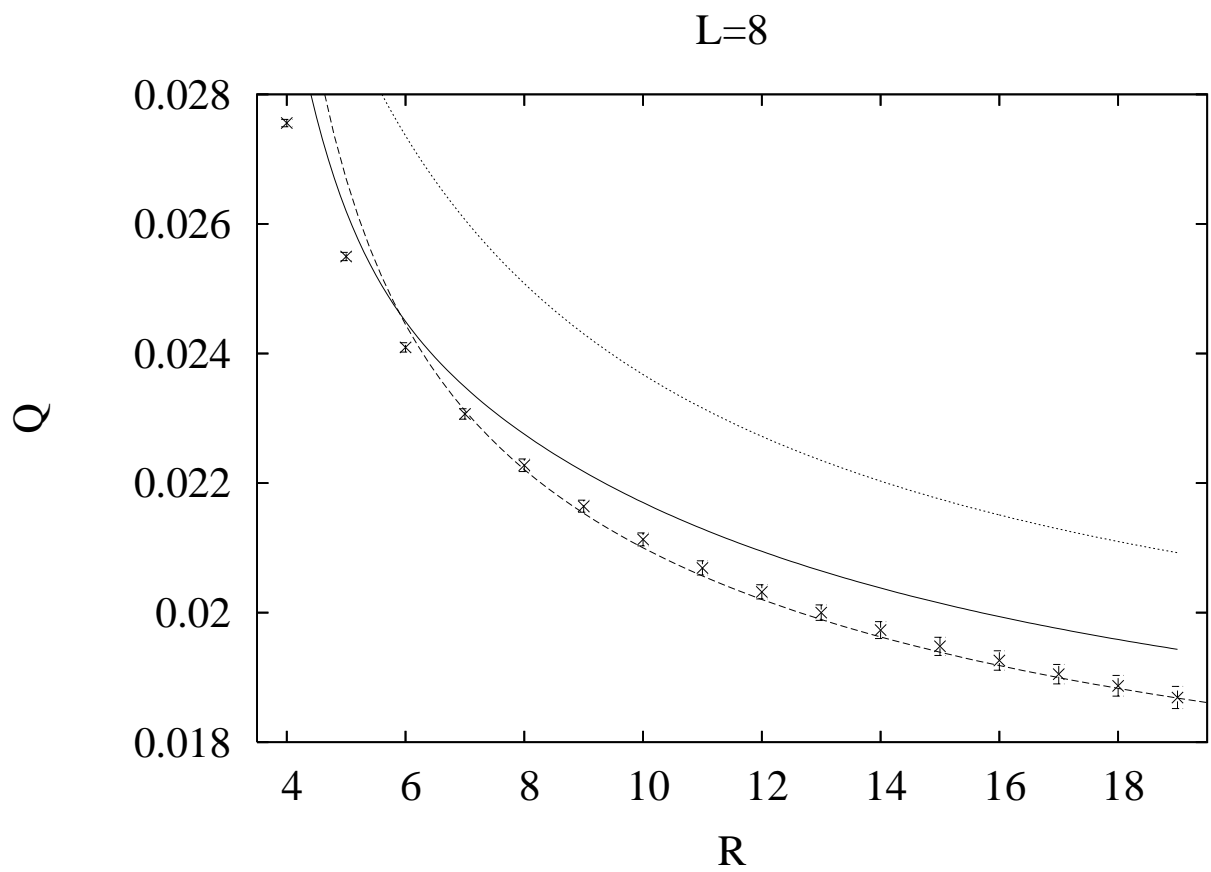


Figure 4: Values of $Q(R)$ for the full Nambu–Goto action (dashed line), the NLO approximation (solid line), the LO approximation (dotted line) and the Monte Carlo results (crosses) for the sample at $\beta = 9.0$, $L = 8$ in the $SU(2)$ model (data of tab. 7).

L	1 loop	2 loop	full NG	MC data
9	0.94940	0.96772		0.96651(22)
10	0.93401	0.94732	0.98210	0.94670(15)
11	0.91984	0.92984	0.93933	0.92915(19)
12	0.90661	0.91433	0.91910	0.91444(18)
13	0.89411	0.90021	0.90295	0.90051(17)
14	0.88221	0.88712	0.88882	0.88752(12)
15	0.87080	0.87482	0.87593	0.87532(11)
16	0.85981	0.86315	0.86390	0.86371(16)
17	0.84917	0.85199	0.85251	0.85252(10)
18	0.83884	0.84124	0.84161	0.84143(10)
19	0.82879	0.83086	0.83113	0.83119(10)
20	0.81899	0.82078	0.82098	0.82102(09)
24	0.78181	0.78291	0.78297	0.78311(11)

Table 5: *Same as table 1, but for a fixed value of R : $R = 32$ and various values of L .*

4 Conclusions

The pattern emerging from the comparisons discussed in the previous section can be summarized in the following points.

- The Nambu–Goto action describes Monte Carlo data rather well for large values of L and R ; however, in this regime it is almost indistinguishable from its truncation at NLO and (for very large values of R) from the pure free bosonic effective string. Nevertheless, it is interesting to note that results from our simulations of the Ising gauge theory at fixed R ($R = 32$ in our case) show that the predictions of the full Nambu–Goto action match the numerical data in the range $L \geq 16$, and in particular there exists a window ($16 \leq L \leq 20$) where the full-order and the NLO-truncated predictions can be clearly distinguished — while for larger values of L this is not possible anymore, within our statistical precision.
- At low temperatures, a common pattern for the three models is observed as R decreases: clear evidence of a mismatch with respect to the string expectation is found. Such a mismatch is increasingly severe for shorter and shorter interquark distances and is not fixed by keeping into account subleading corrections beyond the NLO approximation of the Nambu–Goto string action. This observation has two relevant consequences. First, at short distances the string spectrum must be different from the Nambu–Goto one, in agreement with the recent observations of [13, 14]. Furthermore, the short distance behaviour seems to disagree with the results obtained in [6] by imposing the open-closed string duality of the effective string. In fact in [6] it was shown that in $d = 2 + 1$ the NLO contribution to the energy levels is fixed

R	LO	NLO	full NG	MC data
2	0.047717	0.076813		0.040455(7)
3	0.036808	0.043891		0.034374(10)
4	0.032445	0.034967	0.037080	0.031426(12)
5	0.030263	0.031378	0.031842	0.029785(14)
6	0.029017	0.029584	0.029731	0.028777(16)
7	0.028237	0.028556	0.028614	0.028113(17)
8	0.027718	0.027910	0.027936	0.027654(19)
9	0.027354	0.027477	0.027490	0.027322(22)
10	0.027090	0.027172	0.027179	0.027076(24)
11	0.026892	0.026949	0.026953	0.026887(28)
12	0.026739	0.026780	0.026782	0.026739(33)
13	0.026619	0.026649	0.026651	0.026616(40)

Table 6: Monte Carlo results (rightmost column) for $Q(R)$ in $SU(2)$ gauge theory at $\beta = 9.0$ and $T = \frac{T_c}{10}$ (corresponding to $L = 60$) in comparison with the theoretical expectations from the LO (second column), NLO (third column) and full (fourth column) effective Nambu–Goto action.

and must coincide with the Nambu–Goto one. This implies (see the derivation in the Appendix) that also the NLO contribution to the interquark potential must be the Nambu–Goto one for any effective string theory fulfilling open-closed string duality. A possible interpretation of these two observations is that at these scales (despite the fact that the leading order Lüscher term still correctly describes the gross features of the interquark potential) there is a breakdown of the effective string picture [13, 14].

- For lower values of L (i.e. as the deconfinement temperature is approached) the situation seems to change, and the effective string picture appears to provide a better description of Monte Carlo data as T approaches T_c . However, there is a relevant difference between the behaviour observed in the \mathbb{Z}_2 and in the $SU(2)$ gauge models: for the Ising gauge model, data are in better agreement with the NLO-truncated than with the full partition function predictions, whereas for the $SU(2)$ theory, the whole Nambu–Goto action appears to provide a remarkably good description of the numerical results.
- However, it is important to stress that this agreement could well be only a coincidence. In fact, dimensional reduction and the Svetitsky–Yaffe conjecture [35] suggest a critical index for the deconfinement transition (both for the Ising and for the $SU(2)$ model) equal to the one of the 2d spin Ising model, i.e. $\nu = 1$. This means:

$$\sigma(T) \sim \sigma_0(T - T_c) \tag{26}$$

On the contrary, from the Nambu–Goto action we find $\nu = 1/2$ [31, 32]. This suggests

R	LO	NLO	full NG	MC data
2	0.04769	0.07537		0.03741(4)
3	0.03660	0.04001		0.03093(5)
4	0.03185	0.02992	0.03179	0.02756(6)
5	0.02915	0.02620	0.02670	0.02550(6)
6	0.02736	0.02449	0.02445	0.02409(7)
7	0.02607	0.02348	0.02312	0.02307(8)
8	0.02508	0.02275	0.02221	0.02227(9)
9	0.02430	0.02218	0.02153	0.02164(9)
10	0.02368	0.02170	0.02100	0.02113(10)
11	0.02316	0.02129	0.02057	0.02069(11)
12	0.02272	0.02095	0.02020	0.02032(11)
13	0.02235	0.02064	0.01990	0.02000(12)
14	0.02203	0.02038	0.01962	0.01973(13)
15	0.02175	0.02015	0.01939	0.01948(14)
16	0.02151	0.01994	0.01918	0.01926(15)
17	0.02129	0.01975	0.01900	0.01905(15)
18	0.02110	0.01958	0.01883	0.01887(16)
19	0.02092	0.01943	0.01868	0.01869(17)

Table 7: *Same as in table 6, but for $T = \frac{3}{4}T_c$ ($L = 8$).*

that at some stage there should be a truncation of the square root expansion in the Nambu–Goto effective string. The order of the power at which this truncation occurs needs not to be universal and can be inferred by looking at the critical temperature. In the Nambu–Goto model in $d = 2 + 1$ dimensions, T_c is expected to be [31, 32]:

$$\frac{T_c}{\sqrt{\sigma}} = \sqrt{\frac{3}{\pi}} \simeq 0.977 \quad (27)$$

This prediction does not agree with the high precision results obtained in [34] for the \mathbb{Z}_2 gauge model $\frac{T_c}{\sqrt{\sigma}} = 1.237(3)$. If one evaluates the order at which the Nambu–Goto expansion should be truncated in order to obtain this value for the critical temperature one finds with a good approximation a quartic polynomial, i.e. one expects to describe well the data with the leading and next to leading order only, as we saw in the previous section. This is particularly evident if one looks at the data collected in tab. 5⁴. On the contrary in the $SU(2)$ case the estimate for T_c is closer to the value predicted by the Nambu–Goto model. The most accurate estimate is

⁴Notice however that it is rather non trivial and in principle unexpected the fact that the linear critical behaviour expected for the model is exactly realized (from a numerical point of view) truncating the Nambu–Goto action and not with a completely different coefficient in front of the quartic term.

R	LO	NLO	full NG	MC data
2	0.0555706	0.0778972		0.0508627(32)
3	0.0446623	0.0500971	0.0592690	0.0434942(32)
4	0.0402990	0.0422344	0.0432510	0.0399646(33)
5	0.0381173	0.0389728	0.0392195	0.0380274(35)
6	0.0368707	0.0373058	0.0373874	0.0368546(38)
7	0.0360915	0.0363358	0.0363683	0.0360941(41)
8	0.0355721	0.0357196	0.0357344	0.0355749(45)
9	0.0352084	0.0353027	0.0353102	0.0352080(49)
10	0.0349440	0.0350071	0.0350111	0.0349401(55)
11	0.0347457	0.0347895	0.0347917	0.0347382(62)
12	0.0345931	0.0346244	0.0346258	0.0345838(73)
13	0.0344732	0.0344962	0.0344970	0.0344673(92)

Table 8: Comparison between theoretical predictions and numerical results for the $SU(3)$ model in $d = 2 + 1$ dimensions obtained from data published in [5]. Results refer to $\beta = 20.0$, $L = 60$ (corresponding to $T \simeq \frac{T_c}{10}$). The format is the same as for table 6 .

(for a recent review with updated estimates see [36]) $\frac{T_c}{\sqrt{\sigma}} = 1.12(1)$, corresponding to much a higher order in the truncation and, accordingly, a better agreement with the prediction of the all-order Nambu–Goto prediction.

The picture which emerges is that the Nambu–Goto action is most probably the correct effective description for large enough values of R and L (see in particular the data collected in tab. 5). However, for different reasons, as R or L are decreased this effective description looses its validity. When R is decreased (most probably due to the anomaly problem discussed in sect. 2) the effective string picture as a whole seems to be no longer valid. When L is decreased the Nambu–Goto string which predicts mean field critical indices must necessarily break down and we observe a crossover towards a new string behaviour (which is different for different gauge groups) with a critical behaviour compatible with that expected from dimensional reduction and the Svetitsky–Yaffe conjecture. In particular, in the two cases that we studied: \mathbb{Z}_2 and $SU(2)$, this effective string seems to be a suitable truncation of the whole Nambu-Goto action. Summarizing these observations we could look at the Nambu-Goto action as a sort of “mean field effective string” which turns out to be a remarkably good approximation for distances larger than a few times the bulk correlation length of the model.

In this respect it would be very interesting to extend the high temperature analysis also to the $SU(3)$ gauge model, running low L simulations like to the ones presented in [12] for the $SU(2)$ gauge group. In fact in the $SU(3)$ case we have (see [36]) $\frac{T_c}{\sqrt{\sigma}} = 0.98(2)$, i.e. an almost perfect agreement of the critical temperature with the Nambu-Goto expectation. Moreover in the $SU(3)$ case the truncation mechanism suggested above should not work

since in this case we expect a non-integer critical index for the deconfinement transition (which according to the Svetitsky–Yaffe conjecture should belong to the 2d \mathbb{Z}_3 universality class).

Acknowledgements. This work was partially supported by the European Commission TMR programme HPRN-CT-2002-00325 (EUCLID). M. P. acknowledges support received from Enterprise Ireland under the Basic Research Programme.

A Partition function truncated at LO and NLO

We show the matching between the full partition function eq. (16) and the LO- and NLO-truncated approximations eq. (8) and eq. (11) respectively.

The square root appearing in the open string spectrum eq. (15) can be expanded perturbatively in powers of $(\sigma R^2)^{-1}$:

$$E_n(R) = \sigma R + \frac{\pi}{R} \left(n - \frac{1}{24} \right) - \frac{\pi^2}{2\sigma R^3} \left(n - \frac{1}{24} \right)^2 + O(\sigma^{-2} R^{-5}) \quad (\text{A.1})$$

Truncating at the first non-trivial order yields:

$$E_n^{LO}(R) = \sigma R + \frac{\pi}{R} \left(n - \frac{1}{24} \right) \quad (\text{A.2})$$

and, correspondingly, the leading-order truncation of the partition function eq. (16) reads:

$$Z^{LO}(R, L) = e^{-\sigma RL} e^{+\frac{\pi}{24} \frac{L}{R}} \sum_{n=0}^{\infty} P(n) e^{-\frac{\pi L n}{R}} \quad (\text{A.3})$$

Defining: $q \equiv 2\pi i\tau$, with $\tau = iu = i\frac{L}{2R}$, one finds:

$$Z^{LO}(R, L) = e^{-\sigma RL} q^{-\frac{1}{24}} \sum_{n=0}^{\infty} P(n) q^n \quad (\text{A.4})$$

Due to the well-known identity:

$$\frac{1}{\prod_{n=1}^{\infty} (1 - q^n)} = \sum_{n=0}^{\infty} P(n) q^n \quad (\text{A.5})$$

and to Dedekind's function definition eq. (10), we end up with:

$$Z^{LO}(R, L) = \frac{e^{-\sigma RL}}{\eta(iu)} \quad (\text{A.6})$$

in agreement with eq. (8).

On the other hand, truncation of eq. (A.1) at the next-to-leading order yields:

$$E_n^{NLO}(R) = \sigma R + \frac{\pi}{R} \left(n - \frac{1}{24} \right) - \frac{\pi^2}{2\sigma R^3} \left(n - \frac{1}{24} \right)^2 \quad (\text{A.7})$$

Correspondingly, the next-to-leading-order approximation for the partition function reads:

$$Z^{NLO}(R, L) = \frac{e^{-\sigma RL}}{\eta(iu)} \left[1 + \frac{\pi^2 L}{1152\sigma R^3} \frac{1}{G(q)} \sum_{n=0}^{\infty} P(n) q^n (1 - 48n + 576n^2) \right] \quad (\text{A.8})$$

where we defined:

$$G(q) \equiv \sum_{n=0}^{\infty} P(n)q^n \quad (\text{A.9})$$

The non-trivial sums appearing on the r.h.s. of eq. (A.8) can be written as:

$$\frac{1}{G(q)} \sum_{n=1}^{\infty} nP(n)q^n = q \frac{d}{dq} \ln G(q) \quad (\text{A.10})$$

and:

$$\frac{1}{G(q)} \sum_{n=1}^{\infty} n^2 P(n)q^n = q^2 \frac{d^2}{dq^2} \ln G(q) + \frac{1}{G(q)} \sum_{n=1}^{\infty} nP(n)q^n + \left[\frac{1}{G(q)} \sum_{n=1}^{\infty} nP(n)q^n \right]^2 \quad (\text{A.11})$$

On the other hand, by virtue of the identity (A.5):

$$q \frac{d}{dq} \ln G(q) = - \sum_{n=1}^{\infty} q \frac{d}{dq} \ln(1 - q^n) = \sum_{n=1}^{\infty} \frac{nq^n}{1 - q^n} \quad (\text{A.12})$$

For any positive integer l , the following identity holds:

$$\sum_{n=1}^{\infty} \frac{n^l q^n}{1 - q^n} = \sum_{k=1}^{\infty} \sigma_l(k) q^k \quad (\text{A.13})$$

where $\sigma_l(k)$ denotes the sum of the l -th powers of the positive divisors of k ; this identity can be easily proven by expanding the l.h.s of eq. (A.13):

$$\sum_{n=1}^{\infty} \frac{n^l q^n}{1 - q^n} = \sum_{n=1}^{\infty} n^l \sum_{k=1}^{\infty} q^{nk} = \sum_{k=1}^{\infty} \left(\sum_{d|k} d^l \right) q^k = \sum_{k=1}^{\infty} \sigma_l(k) q^k \quad (\text{A.14})$$

where $\sum_{d|k}$ is precisely the sum over positive divisors of k . Using the identity (A.13) and the definition of the Eisenstein function eq. (12), one gets:

$$q \frac{d}{dq} \ln G(q) = \frac{1 - E_2(q)}{24} \quad (\text{A.15})$$

Finally, the terms in (A.11) can be handled using the fact that:

$$q^2 \frac{d^2}{dq^2} = q \frac{d}{dq} q \frac{d}{dq} - q \frac{d}{dq} \quad (\text{A.16})$$

and the following identity among Eisenstein functions:

$$q \frac{d}{dq} E_2(q) = \frac{E_2^2(q) - E_4(q)}{12} \quad (\text{A.17})$$

which yield:

$$q^2 \frac{d^2}{dq^2} \ln G(q) = \frac{E_4(q) - E_2^2(q)}{288} - \frac{1 - E_2(q)}{24} \quad (\text{A.18})$$

Plugging the various terms into eq. (A.8), one ends up with:

$$Z^{NLO}(R, L) = \frac{e^{-\sigma RL}}{\eta(iu)} \left\{ 1 + \frac{\pi^2 L}{1152\sigma R^3} [2E_4(iu) - E_2^2(iu)] \right\} \quad (\text{A.19})$$

which is exactly eq. (11), as it was expected.

References

- [1] M. Lüscher, K. Symanzik and P. Weisz, Nucl. Phys. **B173** (1980) 365.
M. Lüscher, Nucl. Phys. **B180** (1981) 317.
- [2] O. Alvarez, Phys. Rev. D **24**, 440 (1981).
- [3] K. Dietz and T. Filk, Phys. Rev. D **27** (1983) 2944.
- [4] M. Lüscher and P. Weisz, JHEP **0109** (2001) 010 [arXiv:hep-lat/0108014].
- [5] M. Lüscher and P. Weisz, JHEP 0207 (2002) 049 [arXiv:hep-lat/0207003].
- [6] M. Lüscher and P. Weisz, JHEP **0407** (2004) 014 [arXiv:hep-th/0406205].
- [7] M. Caselle, R. Fiore, F. Gliozzi, M. Hasenbusch, K. Pinn and S. Vinti, Nucl. Phys. B **432** (1994) 590 [arXiv:hep-lat/9407002].
- [8] M. Caselle, R. Fiore, F. Gliozzi, M. Hasenbusch and P. Provero, Nucl. Phys. B **486** (1997) 245 [arXiv:hep-lat/9609041].
- [9] M. Caselle, M. Panero and P. Provero, JHEP **0206** (2002) 061 [arXiv:hep-lat/0205008].
- [10] M. Caselle, M. Hasenbusch and M. Panero, JHEP **0301** (2003) 057 [arXiv:hep-lat/0211012].
- [11] M. Caselle, M. Hasenbusch and M. Panero, JHEP **0405** (2004) 032 [arXiv:hep-lat/0403004].
- [12] M. Caselle, M. Pepe and A. Rago, JHEP **0410** (2004) 005 [arXiv:hep-lat/0406008].
- [13] K. J. Juge, J. Kuti and C. Morningstar, Phys. Rev. Lett. **90** (2003) 161601 [arXiv:hep-lat/0207004].

- [14] K. J. Juge, J. Kuti and C. Morningstar, Nucl. Phys. Proc. Suppl. **129** (2004) 686 [arXiv:hep-lat/0310039].
- K. J. Juge, J. Kuti and C. Morningstar, arXiv:hep-lat/0401032.
- [15] R. Sommer, Nucl. Phys. B **411** (1994) 839 [arXiv:hep-lat/9310022].
- [16] S. Necco and R. Sommer, Nucl. Phys. B **622** (2002) 328 [arXiv:hep-lat/0108008].
- [17] B. Lucini and M. Teper, Phys. Rev. D **64** (2001) 105019 [arXiv:hep-lat/0107007].
- [18] P. Majumdar, Nucl. Phys. B **664** (2003) 213 [arXiv:hep-lat/0211038].
- [19] Y. Koma, M. Koma and P. Majumdar, Nucl. Phys. B **692** (2004) 209 [arXiv:hep-lat/0311016].
- [20] P. Majumdar, arXiv:hep-lat/0406037.
- [21] M. Panero, arXiv:hep-lat/0408002.
- [22] O. Jahn and P. de Forcrand, Nucl. Phys. B (Proc. Suppl.) 129-130 (2004) 700.
- [23] O. Jahn and O. Philipsen, Phys. Rev. D **70** (2004) 074504 [arXiv:hep-lat/0407042].
- [24] J. F. Arvis, Phys. Lett. B **127** (1983) 106.
- [25] Y. Nambu, in *Symmetries and Quark Models*, ed. R. Chand, (Gordon and Breach, New York, 1970).
- [26] T. Goto, Prog. Theor. Phys. **46** (1971) 1560.
- [27] Y. Nambu, Phys. Rev. D **10** (1974) 4262.
- [28] G. H. Hardy and S. Ramanujan, Proc. London Math. Soc. **17** (1918) 75.
- [29] R. P. Stanley “*Enumerative combinatorics*,” Ed. Cambridge studies in Adv. Math. 49.
- [30] P. Olesen, Phys. Lett. **B160** (1985) 144.
- [31] P. Olesen, Phys. Lett. B **160** (1985) 408.
- [32] R. D. Pisarski and O. Alvarez, Phys. Rev. D **26** (1982) 3735.
- [33] M. Caselle and M. Hasenbusch, Nucl. Phys. B **470** (1996) 435 [arXiv:hep-lat/9511015].
- [34] M. Hasenbusch, Int. J. Mod. Phys. C **12** (2001) 991.
- [35] B. Svetitsky and L. G. Yaffe, Nucl. Phys. B **210** (1982) 423.
- [36] H. Meyer and M. Teper, JHEP **0412** (2004) 031 [arXiv:hep-lat/0411039].